Journal of Physics B: Atomic, Molecular and Optical Physics

ACCEPTED MANUSCRIPT

Dynamic effective charge in the continuum on the CDW-EIS model for ionisation in ion-atom collisions: angular and energy dependence.

To cite this article before publication: Maria Fernanda Rojas *et al* 2023 *J. Phys. B: At. Mol. Opt. Phys.* in press https://doi.org/10.1088/1361-6455/acd60d

Dynamic effective charge in the continuum on the CDW-EIS model for ionisation in ion-atom collisions: angular and energy dependence.

M. F. Rojas[†] **M. A. Quinto**[†] **R. D. Rivarola**[†] **J. M. Monti**[†]

[†]Laboratorio de Colisiones Atómicas. Instituto de Física Rosario (CONICET-UNR) and Facultad de Ciencias Exactas, Ingeniería y Agrimensura, Universidad Nacional de Rosario, Avenida Pellegrini 250, 2000 Rosario, Argentina

E-mail: rojas@ifir-conicet.gov.ar

January 2023

Abstract. In this work, a dynamic charge is employed in the Continuum Distorted Wave - Eikonal Initial State theoretical model to describe the non-Coulomb potential of the residual target for single ionisation in bare ion-multielectron atom collisions. A comparison between the well-known Belkić's prescription and the effective charge depending on emission-angle and -energy in the final residual-target continuum state is shown. The obtained results shown that this effective charge improves the description of double differential cross sections for backwards emission angles over the whole emission energy range allowing the calculation of simply differential and total cross sections.

Keywords: Ion-atom collision, Ion-molecule collision, ionisation, Distorted wave, Dynamic charge.

1. Introduction

Understanding the process of single ionisation in ion-atom collisions is of fundamental interest in many different areas like astrophysics, plasma physics, radiation physics and biophysics. In particular, being electron emission the main energy loss mechanism in the interaction of swift ions with matter, it plays a predominant role in applied areas like the design of fusion reactors, radiation damage and radiobiology. For the last mentioned, the knowledge of the differential and total cross sections for single and multiple electronic reactions are necessary to run Monte Carlo simulations of the projectile track and the time evolution of the electrons ejected throughout it. To this end, different semi-empirical and theoretical models are employed. The first are usually fitted to correctly describe existing experimental data, this restricts their range of reliability and they may inherit possible experimental inaccuracies. The latter are derived from first principles and even when they may not perfectly describe the existing experimental data, they are not restricted to experimental availability and they are not affected by possible experimental inaccuracies with the possibility of being improved independently of them.

In that context the Continuum Distorted Wave - Eikonal Initial State model (CDW-EIS) was applied with success to describe numerous collision systems, ranging from bare

multiply charged to fully and partially dressed ions as projectiles, and multielectronic atoms to large biomolecules as targets [1–6]. The computed cross sections, which have been realised within CDW-EIS approximation, for the ionisation of biomolecules by bare ions were used in the TILDA-V, a Monte Carlo code, with the aim of determining the radiobiological end-points such as stopping power, Bragg peak position, and energy deposition [7]. The correct determination of these radiobiological parameters is necessary in the application of important medical treatments as in vectorized radiotherapy. Should be taken into account the fact that the extensive DDCS data (thousands) is fundamental for compute electronic tracks in the Monte Carlo codes used in this type of therapy.

Within the CDW-EIS model, the residual target final continuum state is approximated by a hydrogenic continuum function with a fixed effective charge that has been usually chosen with Belkić's criteria [8]. These criteria relates the effective screened charge of the residual target with the binding energy of the initial bound orbital from which the electron was ionised. However, with this criteria, a systematic underestimation of the backwards emission process is observed. In a previous study [9], it was seen that considering a dynamic effective charge with a linear angular dependence improves the description of double differential cross sections for backward emission angles for high enough emission energies.

The present study is concerned with considering a dynamic effective charge that takes into consideration not only the emission angle but also the emission energy. Therefore being able to calculate simply differential and total cross sections.

Atomic units will be used in the following except when stated otherwise.

2. Theory

We address the problem of single ionisation in ion-atom collisions by means of the CDW-EIS model [10] (see also [11, 12]). The treatment of the multielectronic target is solved by reducing it to a one-electron system in which the passive electrons are considered to remain frozen in their initial orbitals during the collision and the active electron (the one to be ionised) evolves independently of them in an effective Coulomb field of the residual target [13], this could be interpreted as a net ionisation reaction (see [14]). This theoretical model has been widely used to compute differential and total ionisation cross sections for many systems, combining different projectiles and atomic and molecular targets, colliding at intermediate to high non-relativistic impact energies (see [6, 15]). We will work with the *prior* version of the CDW-EIS theory which includes the passive electron dynamic screening over the active one via the initial target bound state (see [1]).

Considering only one active electron, the multielectronic Hamiltonian can be reduced to:

$$H_{el} = -\frac{1}{2}\nabla^2 + V_T(\mathbf{x}) + V_P(\mathbf{s}) + V_s(\mathbf{R}) \tag{1}$$

where $\mathbf{x}$ and $\mathbf{s}$ give the active electron position in the target and projectile reference frames, respectively. $V_T(\mathbf{x})$ is a potential which takes into account the interaction of the active electron with the rest of the target, $V_P(\mathbf{s}) = -Z_P/s$ is the interaction between the bare projectile and the active electron, and $V_s(\mathbf{R})$ the interaction of the projectile with the target nucleus and the passive electrons.

Following Fainstein *et al.* [13], within the straight-line version of the impact parameter approximation, two-centre initial and final distorted-waves are proposed, considering that the electron evolves in the simultaneous presence of both the projectile and residual target fields. Thus, the initial- and final-channel distorted-wave functions are given by:

$$\chi_i^+(\mathbf{x},t) = \Phi_i(\mathbf{x},t)\,\mathscr{L}_i^+(\mathbf{s})\cdot\exp\left[-i\int_{-\infty}^{t} V_s(\mathbf{R})dt'\right] \quad (2)$$

$$\chi_f^-(\boldsymbol{x},t) = \Phi_f(\boldsymbol{x},t)\,\mathscr{L}_f^-(\boldsymbol{s})\cdot\exp\left[+i\int_{t}^{+\infty} V_s(\boldsymbol{R})dt'\right], \quad (3)$$

where

$$\Phi_{i,f}(\mathbf{x},t) = \phi_{i,f}(\mathbf{x})\mathrm{e}^{-i\varepsilon_{i,f}t} \quad (4)$$

are the initial-bound and final-continuum states solutions of the time-dependent target Schrödinger equation, being ε_i the active electron initial binding energy, and $\varepsilon_f = k^2/2$ its energy in the final state. In this formalism, the transition amplitude is given by (see [6, 13]):

$$A_{if} = -i\int_{-\infty}^{+\infty} dt\left\langle \chi_f^- \left| \left(H - i\frac{\partial}{\partial t}\Big|_x\right)\right| \chi_i^+\right\rangle \cdot\exp\left[-i\int_{-\infty}^{+\infty} V_s(\mathbf{R})dt'\right]. \quad (5)$$

Since $V_s(\mathbf{R})$ is independent of the electronic coordinate it contributes to the scattering amplitude through an exponential phase, and so it is relevant for the projectile angular deviation but does not affect the electron dynamics. As we are interested in doubly and singly differential cross sections depending only on the energy and/or angular distributions of the emitted electron and on total cross sections, we discard the contribution of $V_s(\mathbf{R})$ in equation (5), taking into account that the square modulus of the scattering amplitude must be considered in the corresponding calculations [13]. The double differential cross sections can be obtained by integrating the transition amplitude:

$$\sigma(E,\theta) = \frac{d\sigma}{dEd\theta} = -k\int d\boldsymbol{\rho}|A_{if}(\boldsymbol{\rho})|^2, \quad (6)$$

where $\boldsymbol{\rho}$ is the straight line impact parameter [16]. Then, the simple differential cross section as a function of the emission angle and emission energy respectively are:

$$\sigma(E) = \frac{d\sigma}{dE} = \int d\theta\sigma(E,\theta) \quad (7)$$

$$\sigma(\theta) = \frac{d\sigma}{d\theta} = \int dE\sigma(E,\theta) \quad (8)$$

and the total cross section is:

$$\sigma = \int dE\sigma(E) = \int d\theta\sigma(\theta) \quad (9)$$

In the case that fully differential cross sections are calculated, the exponential term in equation (5) must be taken into account. In CDW-EIS the initial distortion is proposed as an eikonal phase:

$$\mathscr{L}_i^+(\mathbf{s}) = \exp\left[-i\nu\ln(vs+\mathbf{v}\cdot\mathbf{s})\right] \quad (10)$$

whereas the final distortion is chosen as:

$$\mathscr{L}_f^-(\mathbf{s}) = N^*(\zeta)\,{}_1F_1(-i\zeta;1;-ips-i\mathbf{p}\cdot\mathbf{s}) \quad (11)$$

where $\mathbf{v}$ is the projectile velocity, $\nu = Z_P/\mathrm{v}$, $\zeta = Z_P/\mathrm{p}$, $\mathbf{p} = \mathbf{k} - \mathbf{v}$ is the ejected electron momentum in the projectile reference frame, $\mathbf{k}$ is the ejected electron momentum in the target reference frame. ${}_1F_1$ is the confluent hypergeometric function, and $N(a) = \exp(\pi a/2)\Gamma(1+ia)$ (with Γ being the Euler's Gamma function) its normalisation factor. The initial bound

orbitals are described by Roothaan-Hartree-Fock (RHF) wavefunctions, which is a well-known numerical method, with large enough data already existing for atoms and ions [17]. In the case of hydrogen atoms, their exact bound wavefunctions can be used. The final continuum wave function in the case of monoelectronic targets is the exact hydrogenic continuum function given by:

$$\phi_f(\mathbf{x}) = \frac{1}{(2\pi)^{3/2}} \exp(i\mathbf{k}\cdot\mathbf{x}) N^*(\lambda)\, {}_1F_1\left[-i\lambda, 1, -i\,(kx+\mathbf{k}\cdot\mathbf{x})\right], \tag{12}$$

with $\lambda = Z_T/k$ being Z_T the target nuclear charge [18]. For multielectronic targets, the non-Coulomb potential of the residual target is usually approximated by an effective Coulomb one [13]. The equation (12) is therefore maintained but with $\lambda = \tilde{Z}_T/k$, where $\tilde{Z}_T$ has been chosen with Belkić's criteria $\tilde{Z}_T = n_i\sqrt{-2\varepsilon_i}$, where n_i is the principal quantum number of the initial bound orbital [8]. The latter expression relates the effective screened charge of the residual target with the binding energy of the initial bound orbital from which the electron was ionised. In others works within a three-body CDW-EIS approximation, more elaborated calculations were developed through the introduction of an exact numerical residual target continuum state in place of the above-mentioned effective Coulombic continuum. In this sense, the one-electron bound and continuum target eigenstates were calculated considering the same Hartree-Fock (HF) target potential, and numerically solving the corresponding target Schrödinger equation [6, 19]. These calculations lead to larger computational time.

The use of a hydrogenic continuum function allows analytical expressions for the transition amplitude but it has some limitations in describing the physics of the reaction. For instance, using this approximation an underestimation of the doubly differential cross sections (DDCS) for backwards angles of the ionised electron is observed. This underestimation was studied by Monti *et al.* [1] in the collision system H^+ on He. Based on the fact that the active electron must deeply penetrate the cloud of passive target electrons in order to impact the target nucleus to be ejected in the backwards direction (see [11]), they proposed to approximate the non-Coulomb potential as a pure Coulomb one given by the target nuclear charge Z_T. By doing so they have observed that the DDCS calculations converged to the ones obtained when using numerical wavefunctions for large scattering angles [1].

In a previous work [9], we explored a dynamic charge defined as a function of the emission angle θ as

$$\tilde{Z}_T(\theta) = Z_B + (Z_T - Z_B)\,\theta/180 \tag{13}$$

with

$$\lim_{\theta\to 0} \tilde{Z}_T(\theta) = Z_B \qquad \text{and} \qquad \lim_{\theta\to 180} \tilde{Z}_T(\theta) = Z_T \tag{14}$$

with Z_B the Belkić charge (mentioned above) and Z_T the target nuclear charge. In this work, we present a dynamic charge defined as a function not only of the emission angle θ but also as a function of the emission energy ε.

We define the function $\tilde{Z}_T(\theta,\varepsilon)$ in terms of Bézier functions [20], as:

$$\tilde{Z}_T(\theta,\varepsilon) = \sum_{i=0}^{m} \binom{m}{i} P_i (1-t)^{m-i} t^i \tag{15}$$

with $t = \theta/180$. Also, P_i is the i-th node of the Bézier curve composed by an angle θ_i and the corresponding charge Z_i, which in a Cartesian plane θZ can be represented by a point of coordinates (θ_i, Z_i), and m the total number of nodes. Each curve is defined by a number of 13 nodes ($m = 12$) chosen as indicated in table 1.

Table 1: Recommended values for θ_i and Z_i.

i	θ_i (degrees)	Z_i
0	0	Z_B
$1-3$	$\theta_{BE}/2$	Z_B
$4-8$	θ_{BE}	Z_B
$9-11$	$(2\times 180+\theta_{BE})/3$	Z_ε
12	180	Z_ε

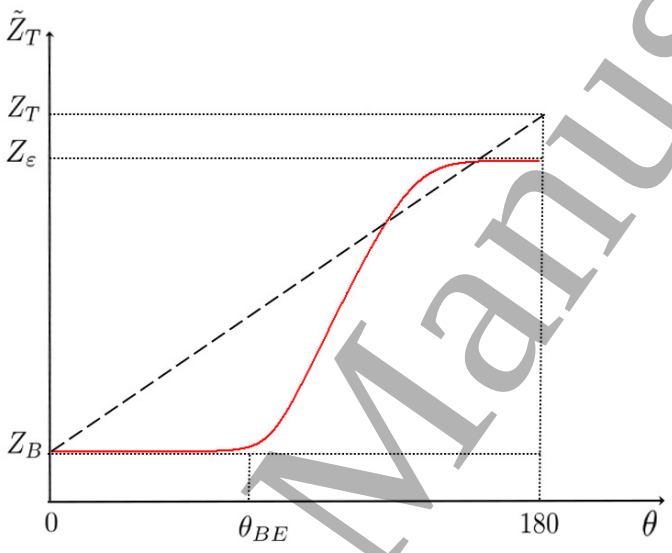

Figure 1: Qualitative behaviour of the effective charge as a function of the emission angle. Black dash-line, dynamic charge depending on the emission angle as in [9]; red line, present dynamic charge as defined in equation (15).

The angle θ_{BE} corresponds to the angular position of the binary encounter peak and it can be found through energy and momentum conservation rules, which predict that in a collision of a bare projectile with a free electron at rest, the binary encounter peak has a maximum at an electron momentum corresponding to $k = 2v\cos\theta_{BE}$ [11]. The behaviour of the dynamic charge, defined as in equation (15), is shown qualitatively in figure 1.
The charge for backward emission angle Z_ε depends explicitly on the emission energy by:

$$Z_\varepsilon = Z_B + (Z_T - Z_B)\cdot\left(1-\mathrm{e}^{-\varepsilon/n_i|\varepsilon_i|}\right), \tag{16}$$

this gives a charge equal to Z_B for low emission-energy and then asymptotically approaches Z_T as the emission energy increases.

The choice for the dynamic charge as defined in equation (15) allows us to take into account two things: first, a slow increment of the effective charge with the emission angle until the binary encounter peak and rapidly increasing afterwards; and second the effective charge for backward emission ($\theta = 180°$) has to increase with the emission energy ε, this given by the assumption that, as emission energy increases, the electron must penetrate closer to the target nucleus in order to be scattered in the backward direction.

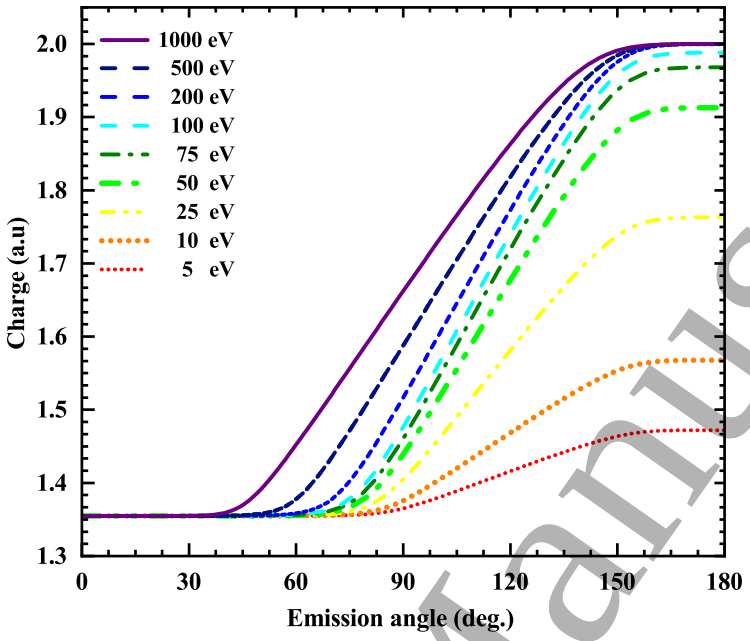

Figure 2: Effective charge as a function of the electron angle of He by the impact of 1 MeV/u H^+. Colour lines show different values of emission energy for the same collision system using the parameters recommended in table 1 for present DC-CDW-EIS.

The recommended values for θ_i and Z_i shown in table 1 have been tested in several cases, being the tabulated values the ones that generated the best results. As an example, figure 2 shows the present dynamic charge as a function of the emission angle for different emission energies for the H^+ + He system at 1 MeV impact energy. It can be seen that the angle θ_{BE} decreases as the emission energy increases given that the angular position of the binary encounter peak shifts to lower angles for higher emission energies. In addition, it can be observed how Z_ε increases with increasing emission energy, as defined by equation (16).

3. Results and Discussions

In this section comparisons between theoretical and experimental DDCS for the ionisation of atomic multielectronic targets are shown. In addition, the singly differential cross sections (SDCS) and total cross sections (TCS) are also analysed. Calculations are performed using DC-CDW-EIS (Dynamic Charge–Continuum Distorted Wave–Eikonal Initial State) models, CDW-EIS model with Belkić's charge and CDW-EIS with numerical HF wavefunctions following the work described in [21].

In figure 3, are presented the single ionisation DDCS as a function of the angular distributions for He impacted by 200 keV proton. For the case of forward emission, all theoretical models give similar results and an overestimation of the experimental DDCS taken

from [22] can be seen for emission energies larger than 25 eV. Nevertheless, it can also be seen that an excellent agreement is obtained when compared to the data taken from [23]. For backward emission, it can be seen that the results from the present and previous DC-CDW-EIS from [9] model, and those obtained using CDW-EIS with numerical functions are in very good agreement with experiments up to an emission energy of 80 eV. On the other hand, the CDW-EIS ones with Belkić's charge present an underestimation that gets larger as the emission energy increases. Nonetheless, for the 200 eV and 300 eV cases, all models still show an underestimation of the experimental DDCS. For the latter, there is almost an order of magnitude between theoretical and experimental DDCS. Also, both DC-CDW-EIS models are in close agreement with the CDW-EIS with numerical functions one. For this system, as discrepancies with experiments still remain, we also added calculations performed for ionization of He by neutral H^0 impact considering the present target dynamic charge into the dressed-ion model presented by Esponda *et al.* (see [24]). This was done in order to enquire if a two-step process in which the proton captures an electron and then ionizes the remaining one, could be responsible for the increase observed in DDCS for high emission energies and emission angles. Even though further investigation regarding this is required, this holds the hypothesis that a two-step process could be taking place.

In figure 4, the angular distributions of the DDCS, at different electron energies, for ionisation of Ne by 5 MeV/u C^{6+} impact are presented. For the lowest emission energy, i.e. 20 eV, the best agreement with experiments is found for the present DC-CDW-EIS model. For that energy, the results obtained with the DC-CDW-EIS model from [9] show an underestimation for emission angles larger than 60 degrees, due to the fact that the linear dynamic charge grows too fast with the emission angle (see figure 1). This shows that a simple linear dynamic charge as proposed in [9] can give good results for DDCS at high enough emission energies but, as will be analysed later, can not be used for calculating SDCS and TCS. For the other displayed emission energies, 200 eV and 520 eV, the behaviour is similar: both DC-CDW-EIS models are close to each other, presenting an underestimation for forward emission but excellent agreement with experiments for emission angles larger than 45 degrees, whereas the usual CDW-EIS model tends to underestimate the experiments for emission angles larger than 90 degrees and, as was seen before, the underestimation increases with the emission energy. The CDW-EIS with numerical functions presents a very good overall agreement with experiments with an overestimation for large emission angles.

In figure 5, it is depicted the ionisation DDCS for proton impinging on Ar, for two collision energies 500 keV/u and 1 MeV/u. For both impact energies, it is clearly seen that the usual CDW-EIS model with the effective charge given by Belkić's criteria only gives good results for low enough emission energies, for larger energies it largely underestimates the experimental DDCS for emission angles larger than the one corresponding to the binary encounter peak. For large emission angles, both DC-CDW-EIS models are in very good agreement with experimental data and with the numerical CDW-EIS, although showing a different behaviour from the last ones for backward angles.

In figure 6, differential cross sections are shown for bare carbon ions and protons colliding with oxygen atoms at impact energies of 5.5 MeV/u C^{6+} and 200 keV/u H^+, respectively. The experimental data correspond to the ionisation of oxygen molecules, as the calculations correspond to atomic oxygen the experimental data was divided by a factor of two in order to perform a qualitative comparison. For the 5.5 MeV/u C^{6+} (figure 6 (a)), the best agreement with the experiments is obtained by the numerical CDW-EIS theory. The present DC-CDW-EIS model also shows good agreement although some underestimation of experiments is found in the 340 eV emission energy case for forward and backward emission angles. As seen before, the previous DC-CDW-EIS from [9] is in accord with

present DC-CDW-EIS calculations only for large enough emission energies, showing an underestimation of experimental data for the lowest emission energy of 11 eV and large emission angle. Finally, the usual CDW-EIS calculations with an effective charge given by Belkić's prescription show the largest underestimation for backward emission. In figure 6 (b) the 200 keV/u H^+ impact energy case is presented. For forward emission, all models show overestimation on all emission energies considered. Nevertheless, for backward emission they are all in very good agreement with the experimental data; except for the results obtained with the usual CDW-EIS model, which shows major underestimation for large emission angles. It can be clearly observed that the overall agreement between theoretical calculations and experiments is much better in the case of 5.5 MeV/u C^{6+}. Taking into account that in both cases the calculations are performed for oxygen atoms, the molecular nature of O_2 seems to be more important for lighter projectiles and lower collision energies.

The ionisation SDCSs as a function of emission angle for Ne and Ar atoms are presented in figure 7. It must be noted that a linear scale is used to represent SDCS. As these SDCS are obtained by integrating the DDCS over the emission energy and given the fact that DDCS decrease as the emission energy increases, it is expected that SDCS are to be largely influenced by the low-energy part of the DDCS spectra. For the 5 MeV/u C^{6+} impinging over Ne targets, figure 7 (a), good agreement with experiments is found for the usual CDW-EIS and the present DC-CDW-EIS one. These two models give almost the same results up to an emission angle of 120 degrees, approximately, after which the usual CDW-EIS model starts to overestimate both the experimental SDCS results and the present DC-CDW-EIS ones. This same behaviour was observed in the DDCS (see figure 4, 20 eV). Then, in figure 7 (b), the SDCS as a function of the emission angle for ionisation of Ar atoms by 0.5 MeV protons impact is shown. The calculations using the usual CDW-EIS and the present DC-CDW-EIS one are in close agreement with each other and give good qualitative agreement with experiments. For both systems, the previous version of DC-CDW-EIS from [9] show the worst agreement. As it was previously mentioned the linear version of the dynamic charge only gives good results for high-energy DDCS, so it is expected to fail when integrating the DDCS on the emission energy to obtain the SDCS.

Finally, in figure 8, the TCS for single ionisation of He, Ne and Ar atoms by H^+ impact is depicted. It is clearly observed that no further agreement is achieved when considering the present dynamic charge compared with the usual CDW-EIS calculations. As expected, given the lack of agreement found for the SDCS, the previous dynamic charge from [9] also shows a large disagreement with experimental data. The present TCSs show good accordance with the experimental data for a collision energy larger than 25 keV, which for this case is actually the impact energy corresponding to a Sommerfeld factor equal to 1.

4. Conclusions

A dynamic effective charge in the residual-target continuum final state on the CDW-EIS model is used to describe single ionisation in ion-atom collisions. The results show that the use of the present effective charge provides an important improvement in the DDCS over the whole emission energy range, which represents an upgrade regarding the previous effective charge proposed in [9] which was only valid for high enough emission energies. Even though DDCS agreement is enhanced, mainly for backward emission, the low energy part of DDCS is mostly unchanged with respect to the usual CDW-EIS model. This translates into a minor gain on the SDCS spectra, whereas the TCS are unchanged when comparing with the usual CDW-EIS calculations using Belkić's prescription.

The cases studied show that the present DC-CDW-EIS model gives results that are close

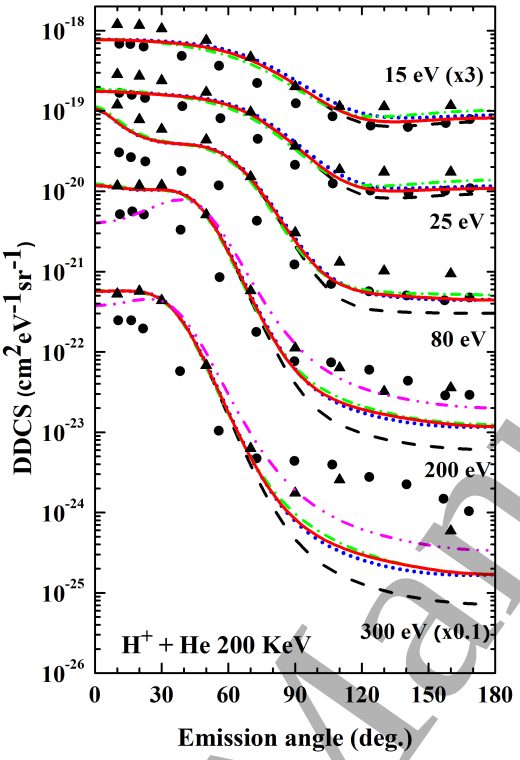

Figure 3: (Color online) DDCS for ionisation of He by the impact of 200 keV/u H^+ for fixed electron energies and as a function of the electron angle. Theory: solid red line present DC-CDW-EIS, dashed black line CDW-EIS, dotted blue line DC-CDW-EIS from [9], dash-dot green line CDW-EIS with numerical functions, dash-dot-dot magenta line present DC-CDW-EIS for H^0 impact. Experiment data: circles [22] and triangles [23].

to those obtained when considering HF numerical wavefunctions, but keeping computation times significantly lower. The DC-CDW-EIS is at least 3.5 times faster than the CDW-EIS with numerical functions. Therefore, the present dynamic effective charge can be used to calculate multiply differential and total cross sections, keeping in mind that the largest improvement will occur on the DDCS, which at the moment is fundamental for the applicability in important medical treatments. The calculation of fully differential cross sections is a matter of our present interest. With this goal in mind an eikonal expression is employed to calculate differential cross sections as a function of the projectile scattering angle has it been done for electron capture by Rivarola and coworkers (see [27]).

Also to reach a further agreement with experiments, a dynamic charge for forward emission should also be considered. This, together with the consideration of the two-step process proposed for the H^+ + He system, will be subjects of future research.

Finally, to improve SDCS and TCS calculations, the low-energy region of the DDCS spectra should be investigated.

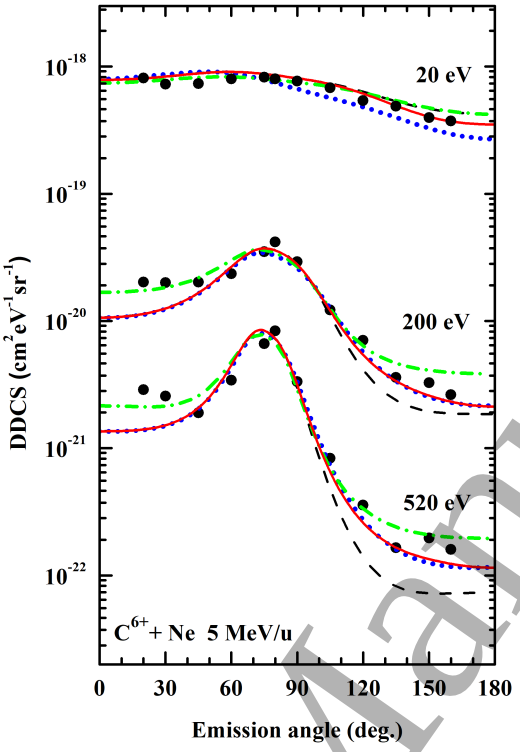

Figure 4: (Color online) Same as figure 3, ionisation of Ne impacted by 5 MeV/u C^{6+}. Experiment data are taken from [2].

Acknowledgments

The authors acknowledge support from the Consejo Nacional de Investigaciones Científicas y Tecnicas de la República Argentina, through Project PIP 2021-3245. The results presented in this work have been obtained by using the facilities of the CCT-Rosario Computational Center, a member of the High-Performance Computing National System (SNCAD, MincyT-Argentina).

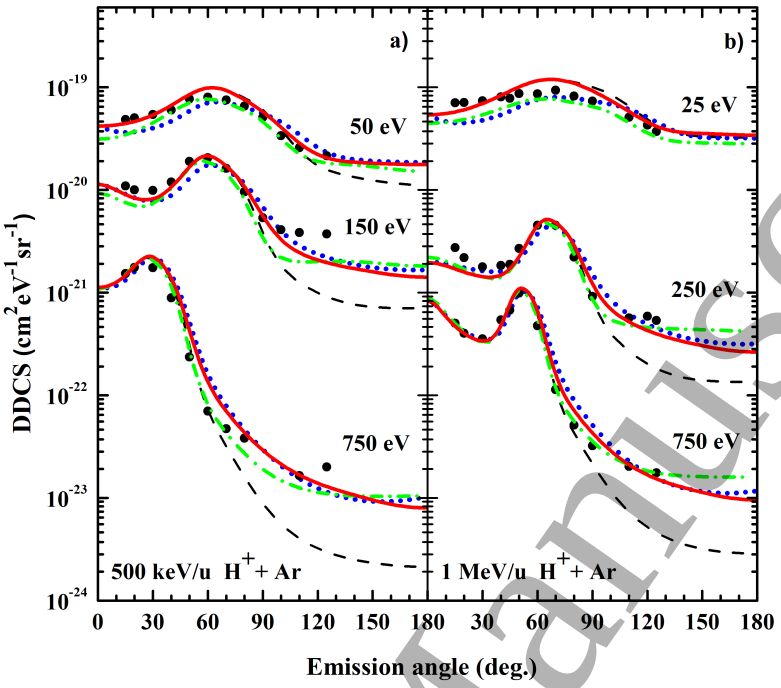

Figure 5: (Color online) Same as figure 3, ionisation of Ar impacted by 0.5 MeV/u H^+ (a) and 1 MeV/u H^+ (b). Experiment data are taken from [25] (data of Toburen).

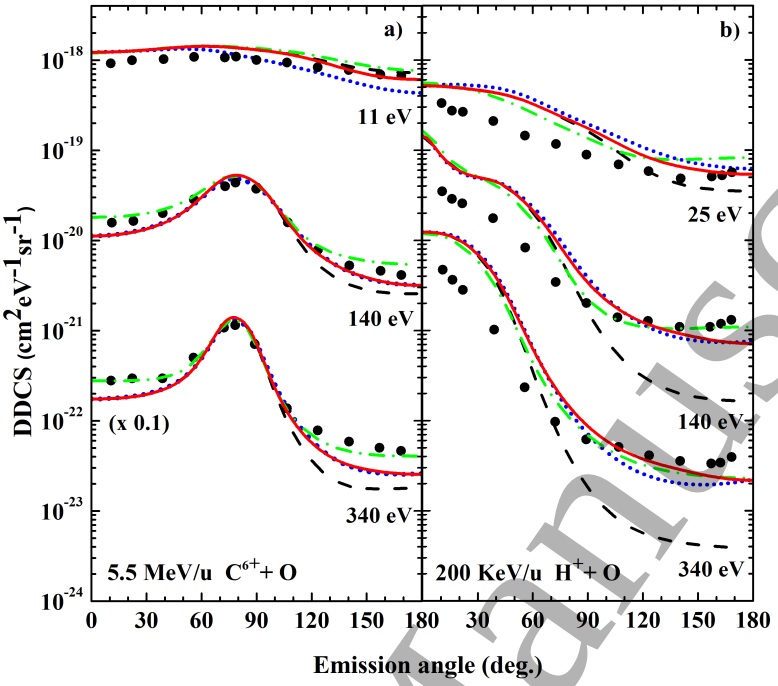

Figure 6: (Color online) Same as figure 3 for ionisation of O atom impacted by 5.5 MeV/u C^{6+} (a) and 200 keV/u H^{+} (b). Experiment data are taken from [22].

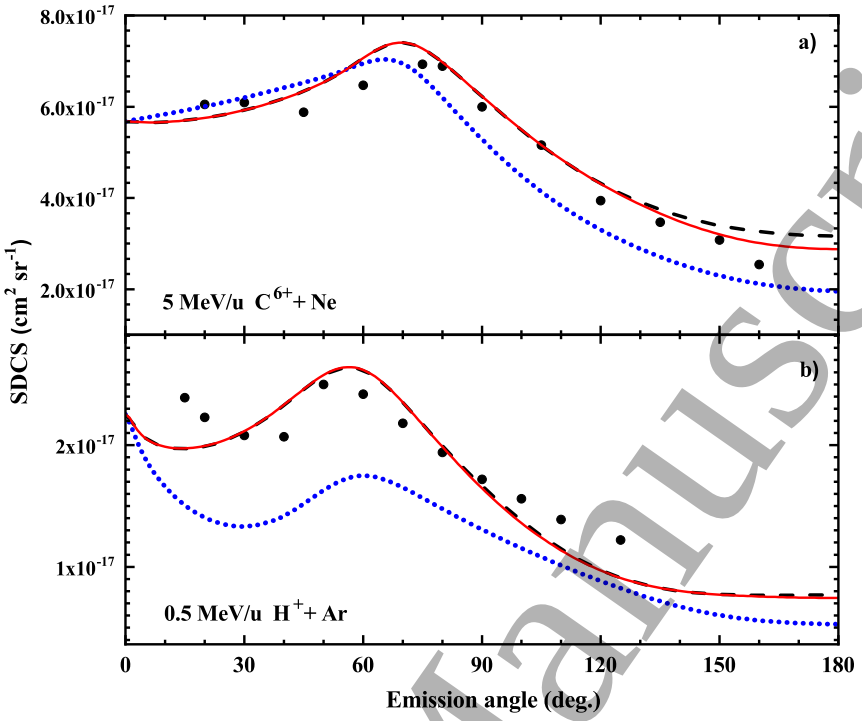

Figure 7: (Color online) SDCS for ionisation of Ne impacted by 5 MeV/u C^{6+} (a) and of Ar impacted by 0.5 MeV/u H^{+} (b) as a function of the electron angle. Theory: solid red line present DC-CDW-EIS, dashed black line CDW-EIS, dotted blue line DC-CDW-EIS from [9]. Experiment data are taken from [2] (a) and [25] (data of Toburen) (b).

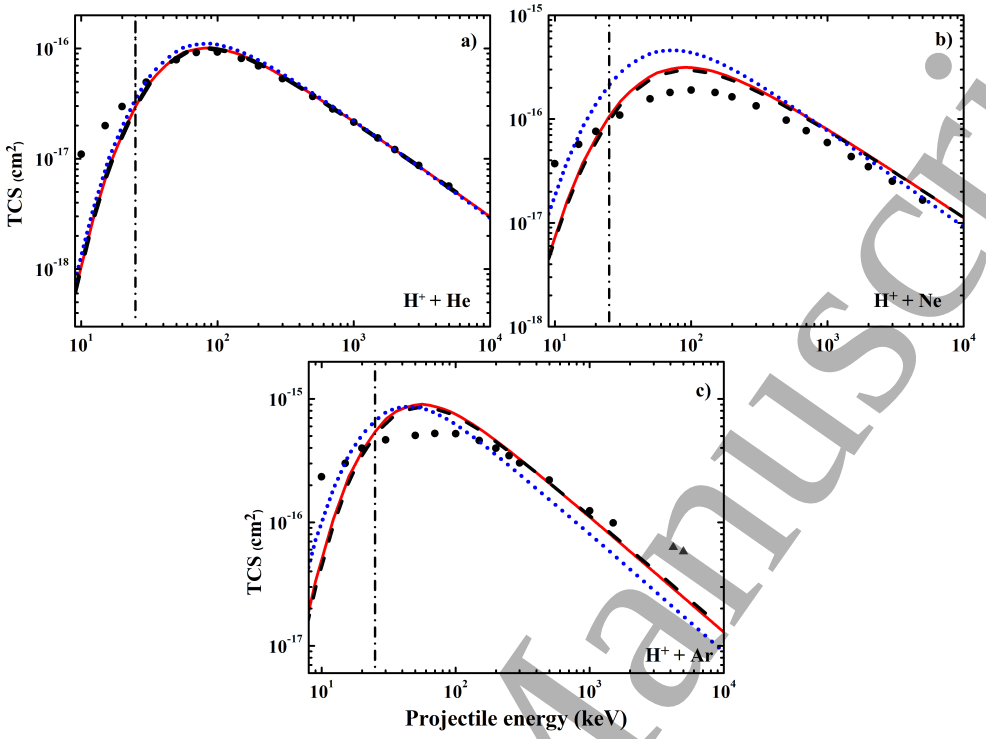

Figure 8: (Color online) TCS for ionisation of He (a), Ne (b) and Ar (c) impacted by H^+ as a function of the projectile energy. Theory: solid red line present DC-CDW-EIS, dashed black line CDW-EIS, dotted blue line DC-CDW-EIS from [9]. Experiment data are taken from [23] (data of Rudd, Toburen and Stolterfoht) (a), [26] (b) and black circles (data of Rudd and Toburen), grey triangles (data of Gabler) [25] (c). The dash-dotted vertical lines represent the lowest collision energy for which the perturbative regime is valid ($Z_p/v = 1$).

[1] J. M. Monti, A. O. Fojón, J. Hanssen, and R. D. Rivarola. Influence of the dynamic screening on single-electron ionization of multi-electron atoms. *J. Phys. B: At. Mol. Opt. Phys.*, 43:205203, 2010.

[2] Shubhadeep Biswas, J. M. Monti, C. A. Tachino, R. D. Rivarola, and L. C. Tribedi. Differential electron emission in the ionization of Ne and Xe atoms under fast bare carbon ion impact. *Journal of Physics B Atomic Molecular Physics*, 48(11):115206, June 2015.

[3] M. E. Galassi, C. Champion, P. F. Weck, R. D. Rivarola, O. Fojón, and J. Hanssen. Quantum-mechanical predictions of DNA and RNA ionization by energetic proton beams. *Physics in Medicine and Biology*, 57(7):2081–2099, April 2012.

[4] J.M. Monti, C.A. Tachino, J. Hanssen, O.A. Fojón, M.E. Galassi, C. Champion, and R.D. Rivarola. Distorted wave calculations for electron loss process induced by bare ion impact on biological targets. *Applied Radiation and Isotopes*, 83:105–108, 2014. Quantum scattering codes and Monte Carlo simulations to model dynamical processes in biosystems.

[5] M. A. Quinto, J. M. Monti, C. Champion, and R. D. Rivarola. Neutral hydrogen versus proton-induced ionization in water vapor. *Phys. Rev. A*, 100(4):042704, October 2019.

[6] L. Gulyas, P. D. Fainstein, and A. Salin. CDW-EIS theory of ionization by ion impact with Hartree-Fock description of the target. *Journal of Physics B Atomic Molecular Physics*, 28(2):245–257, January 1995.

[7] Mario E. Alcocer-Ávila, Michele A. Quinto, Juan M. Monti, Roberto D. Rivarola, and Christophe Champion. Proton transport modeling in a realistic biological environment by using TILDA-V. *Scientific Reports*, 9:14030, October 2019.

[8] D. Belkic, R. Gayet, and A. Salin. Electron capture in high-energy ion-atom collisions. *Phys. Rep.*, 56:279, 1979.

[9] M. F. Rojas, M. A. Quinto, R. D. Rivarola, and J. M. Monti. Dynamic effective charge in the target continuum within the CDW-EIS model for ionisation in ion-atom collisions: angular dependence. *European Physical Journal D*, 75(5):154, May 2021.

[10] D. S. F. Crothers and J. F. McCann. Ionisation of atoms by ion impact. *J. Phys. B: At. Mol. Phys.*, 16:3229–3242, 1983.

[11] N. Stolterfoht, R. D. DuBois, and R. D. Rivarola. *Electron Emission in Heavy Ion-Atom Collisions*. Springer-Verlag Berlin Heidelberg, 1997.

[12] P. D. Fainstein, V. H. Ponce, and R. D. Rivarola. Two-centre effects in ionization by ion impact. *J. Phys. B: At. Mol. Opt. Phys.*, 24:3091–3119, 1991.

[13] P. D. Fainstein, V. H. Ponce, and R. D. Rivarola. A theoretical model for ionisation in ion-atom collisions. Application for the impact of multicharged projectiles on helium. *J. Phys. B: At. Mol. Opt. Phys.*, 21:287–299, 1988.

[14] C. C. Montanari and J. E. Miraglia. Antiproton, proton and electron impact multiple ionization of rare gases. *Journal of Physics B Atomic Molecular Physics*, 45(10):105201, May 2012.

[15] G. C. Bernardi, S. Suárez, P. D. Fainstein, C. R. Garibotti, W. Meckbach, and P. Focke. Two-center effects in electron emission in $^3He^{2+}$-He and H^+-He collisions at intermediate energies. *Physical Review A*, 40(12):6863–6872, December 1989.

[16] M.R.C. McDowell and J.P. Coleman. *Introduction to the Theory of Ion-atom Collisions*. North-Holland Publishing Company, 1970.

[17] E. Clementi and C. Roetti. Roothaan-Hartree-Fock Atomic Wavefunctions: Basis Functions and Their Coefficients for Ground and Certain Excited States of Neutral and Ionized Atoms, Z <= 54. *At. Data Nucl. Data Tables*, 14:177, 1974.

[18] P. D. Fainstein and R. D. Rivarola. Symmetric eikonal model for ionisation in ion-atom collisions. *Journal of Physics B Atomic Molecular Physics*, 20(6):1285–1293, March 1987.

[19] C. C. Montanari and J. E. Miraglia. Ionization probabilities of Ne, Ar, Kr, and Xe by proton impact for different initial states and impact energies. *Nuclear Instruments and Methods in Physics Research B*, 407:236–243, September 2017.

[20] Senay Baydas and Bulent Karakas. Defining a curve as a bezier curve. *Journal of Taibah University for Science*, 13(1):522–528, 2019.

[21] P. D. Fainstein, L. Gulyas, and A. Salin. Angular distribution of electrons ejected from argon by 350 keV proton impact: CDW-EIS approximation. *Journal of Physics B Atomic Molecular Physics*, 27(11):L259–L264, June 1994.

[22] Madhusree Roy Chowdhury, A. Mandal, A. Bhogale, H. Bansal, C. Bagdia, S. Bhattacharjee, J. M. Monti, R. D. Rivarola, and Lokesh C. Tribedi. Ionization of atoms and molecules using 200-kev protons and 5.5-mev/u bare c ions: Energy-dependent collision dynamics. *Phys. Rev. A*, 102:012819, Jul 2020.

[23] M. E. Rudd, L. H. Toburen, and N. Stolerfoht. Differential Cross Sections for Ejection of Electrons from Helium by Protons. *Atomic Data and Nuclear Data Tables*, 18:413, January 1976.

[24] N. J. Esponda, M. A. Quinto, R. D. Rivarola, and J. M. Monti. Dynamic screening and two-center effects in neutral and partially dressed ion-atom collisions. *Phys. Rev. A*, 105:032817, Mar 2022.

[25] M. E. Rudd, L. H. Toburen, and N. Stolterfoht. Differential Cross Sections for Ejection of Electrons from

Argon by Protons. *Atomic Data and Nuclear Data Tables*, 23:405, January 1979.

[26] M. E. Rudd, Y. K. Kim, D. H. Madison, and J. W. Gallagher. Electron production in proton collisions: total cross sections. *Reviews of Modern Physics*, 57(4):965–994, October 1985.

[27] R D Rivarola, R D Piacentini, A Salin, and Dz Belkic. The influence of the static potential in high-energy k-shell electron capture collisions. *Journal of Physics B: Atomic and Molecular Physics*, 13(13):2601, jul 1980.